Real-Time Examination of Atomistic Mechanisms during Shock-Induced Structural Transformation in Silicon

Stefan J. Turneaure, N. Sinclair, and Y. M. Gupta
Institute for Shock Physics and Department of Physics, Washington State University, Pullman, Washington 99164-2816, USA
(Received 18 February 2016; published 20 July 2016)

The experimental determination of atomistic mechanisms linking crystal structures during a compression-driven solid-solid phase transformation is a long-standing and challenging scientific objective. Using new capabilities at the Dynamic Compression Sector at the Advanced Photon Source, the structure of shocked Si at 19 GPa was identified as simple hexagonal, and the lattice orientations between ambient cubic diamond and simple hexagonal structures were related. The approach is general and provides a powerful new method for examining atomistic mechanisms during stress-induced structural changes.

DOI: 10.1103/PhysRevLett.117.045502

Stress- or compression-induced structural changes between different crystal structures have been a central element of both static high-pressure and shock-compression research. Historically, shock wave studies have relied on static pressure results to infer crystal structures at comparable stresses or densities. Despite the large body of static high-pressure and shock wave data to date, molecular dynamics (MD) simulations—a computational approach—offer the only general method to follow atomic motions during a compression-induced structural transformation. For example, MD simulations were used recently to investigate shock-induced structural transformations in materials such as quartz [1] and silicon [2]. However, because of the uncertainties in the interatomic potentials and the small length and time scales that can be examined in MD simulations, there remains a strong need for a general experimental approach to follow atomistic changes or motions during compression-induced structural transformations.

Because a given atomistic transformation pathway results in particular orientation relations between the parent and daughter structures, the experimental determination of such orientation relations provides insight into the atomistic transformation mechanisms. In the present work, we demonstrate that planar shock-compression experiments on single crystals incorporating real-time synchrotron x-ray diffraction (XRD) measurements can be used to examine the orientation relations between parent and daughter structures in single-event experiments, addressing a long-standing need in compression science. Such XRD measurements probing the orientations of the high-pressure structure relative to the ambient structure orientation—under dynamic compression—also provide the data needed to assess the validity of MD simulations of stress-induced structural transformations.

Planar shock-compression experiments are particularly useful for examining stress-induced structural changes, because a macroscopic quantity of material can transform across a planar shock front on nanosecond time scales [3,4]. Furthermore, shock-compressed materials are inertially confined; for shock-compressed single crystals, the inertial confinement is expected to result in a less mosaic high-pressure structure compared with slow compression that occurs in diamond anvil cells. Indeed, XRD measurements on high-pressure structures of shock-compressed KCl [5,6] and Fe [7,8] have found a high degree of preferred orientation for the high-pressure structures and have provided some insight into the atomistic transformation mechanisms. These experimental studies utilized flash x rays [5,6] and laser-based x rays [7,8] resulting in the following experimental limitations: single-pulse measurements lacking temporal evolution, a broad spectrum of undesirable background x rays, and large beam divergence.

The Dynamic Compression Sector (DCS) at the Advanced Photon Source (APS) is a new experimental capability that links dedicated dynamic compression drivers to a third-generation synchrotron light source [9]. Powder guns, a single-stage gas gun, and a two-stage gas gun (all with half-inch bores) can be used to achieve projectile velocities exceeding 5.5 km/s for plane shock-compression experiments. A focused pink x-ray beam (few percent bandwidth, peak energy between 7 and 35 keV), with unwanted higher harmonics filtered out using Kirkpatrick-Baez mirrors, is used for single-pulse XRD images (~100 ps duration) during impact events. A four-frame XRD detector at the DCS allows the study of temporal evolution of structural changes during shock compression and release by recording four XRD frames with an interframe spacing of 153.4 ns.

In this Letter, we describe results from the first XRD experiments using the DCS two-stage gas gun to examine structural changes in shock-compressed silicon. For static pressures up to 38 GPa, silicon undergoes several structural transformations with increasing pressure: ambient cubic diamond (cd) to β-Sn [10–13] (transformation pressure, $P_t = 11.7$ GPa; volume compression, $\Delta V = 21.0\%$) [12] to *Imma* [10,12,14,15] ($P_t = 13.2$ GPa; $\Delta V = 0.2\%$) [12]

to simple hexagonal [10,12,16–18] ($P_t = 15.4$ GPa; $\Delta V = 0.5\%$) [12] to *Cmca* [10,17,19] ($P_t \sim 38$ GPa; $\Delta V = 5.1\%$) [19]. Despite extensive prior examination of structural changes in compressed silicon [10–19], no direct experimental determination of the atomistic transformation mechanisms or the orientation relations between the different silicon polymorphs has been reported to date.

Although shock compression is a promising approach for examining the orientation relations between high-pressure silicon structures, a lack of desired measurements in past work [20–22] has precluded the determination of shocked silicon structure. Analysis of transmitted wave profiles in shocked single-crystal silicon has indicated—through density determination—that a phase transformation begins around 13 GPa [20–22] and that above 16 GPa the density of shocked silicon is consistent with the density of one of the high-pressure crystalline structures observed under static compression [22]. However, a recent post-mortem analysis of recovered laser-shocked Si(100) suggested that amorphization rather than transformation to a high-pressure crystalline structure occurs during shock compression of Si(100) [23]. Additionally, previous XRD measurements on laser-shocked single-crystal silicon with reported stresses greater than the phase transformation stress did not find evidence for any of the high-pressure silicon structures found under static compression [24,25]. Thus, the structure of shock-compressed silicon (crystalline or amorphous) remains an open question.

Using the new real-time XRD capabilities at the DCS, we directly determined the structure of silicon at 19 GPa in plate impact experiments for both polycrystalline and single-crystal samples; the shocked silicon is found to be crystalline with the simple hexagonal (sh) structure. More importantly, our results for shock-compressed single-crystal silicon provide the first direct evidence for the orientation relations between ambient cubic diamond silicon and a high-pressure silicon structure (simple hexagonal).

Figure 1 shows the configuration for plate impact XRD experiments performed on a polycrystalline silicon sample and on single-crystal silicon samples shocked along either [100] or [111]. Flat-faced polycarbonate (PC) projectiles (12.7 mm diameter) accelerated to about 5.1 km/s impacted silicon plates resulting in longitudinal impact stresses of 26 GPa [26], significantly larger than the phase transformation onset stress of 13 GPa [20–22]. The silicon samples were backed by a PC window. Stress waves reverberate through the silicon between the impactor and the window, resulting in a constant state silicon stress of 19 GPa [26]. A framing x-ray area detector was used to record four XRD frames during the impact event with 153.4 ns interframe spacing [26]. In each experiment, one of the frames was obtained while the shocked Si was in a constant 19 GPa state, and we focus our XRD analysis on those results; an additional description of the time evolution

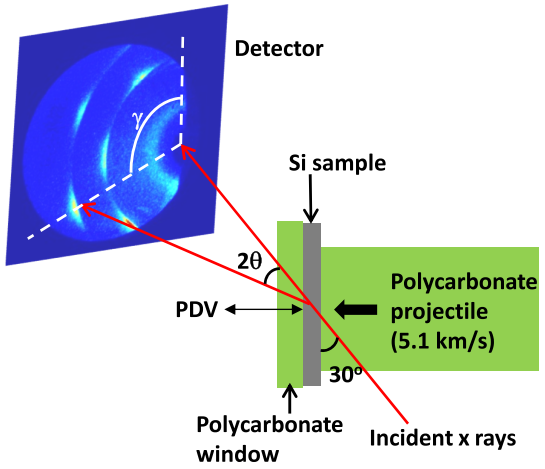

FIG. 1. Configuration for the time-resolved, x-ray diffraction measurements in silicon subjected to impact loading. A PC projectile traveling at ~5.1 km/s impacted the Si samples. Pulsed x rays (~23.5 keV energy, ~100 ps duration, 153.4 ns period) passed through the PC projectile, the silicon sample, and the PC window. Diffracted x rays from individual ~100 ps x-ray pulses were detected on a framing area detector with a 75 mm diameter field of view. Photon Doppler velocimetry (PDV) was used to record the velocity history of the Si/PC interface [26].

of the XRD frames is provided in Supplemental Material [26]. Table S1 lists the experimental parameters [26].

Figure 2 shows representative diffraction images (for the polycrystalline Si sample) obtained in one of the impact experiments. The ambient diffraction pattern for the polycrystalline sample [Fig. 2(a)] exhibits smooth cd structure diffraction rings as expected for a randomly oriented fine-grained polycrystalline sample. In the first frame after impact (99 ns), the original cd diffraction rings are still observed, but new rings also appear, indicating a new crystalline phase; diffraction rings from both phases appear together, because 99 ns after impact the shock wave causing the phase transformation has traveled only through half of the silicon sample [26]. By the third frame after impact (406 ns), the phase transformation wave has propagated through the entire silicon sample, and at least one reflection of this wave has propagated back through the silicon [26]. Thus, at 406 ns after impact, the entire silicon sample is in a constant state: longitudinal stress of about 19 GPa. At this time, the cd structure diffraction rings (ambient phase) are completely absent, and three new diffraction rings are observed showing a full transformation to a high-pressure crystalline structure.

The structure of the polycrystalline Si at 19 GPa was determined by integrating the diffracted intensity around the γ angle [26] to obtain the diffracted intensity vs the 2θ scattering angle and comparing the measured results with diffraction simulations assuming either the β-Sn, *Imma*, or sh structures. The simulation assuming a randomly oriented simple hexagonal structure with lattice parameters $c_{sh} = 2.380(8)$ Å and $a_{sh} = 2.562(8)$ Å best matched the

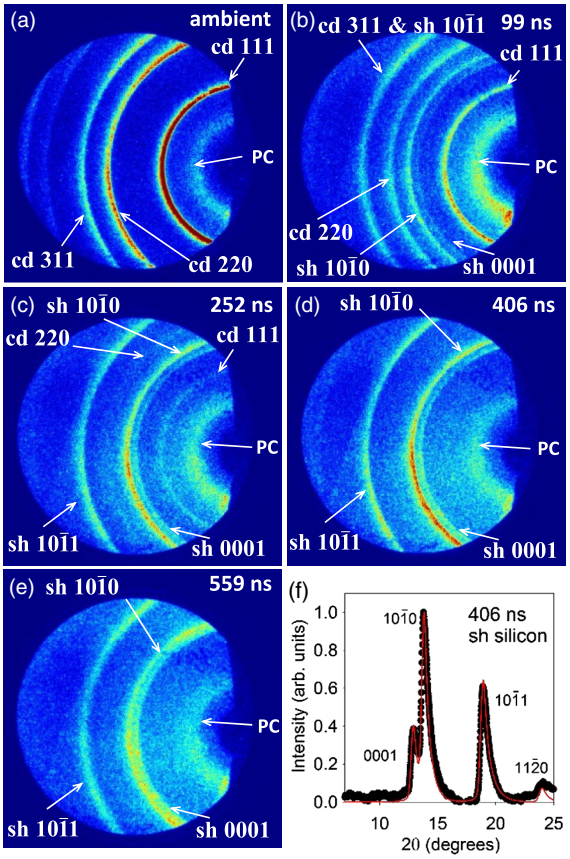

FIG. 2. X-ray diffraction results for shocked polycrystalline silicon. (a) Ambient cd phase Si diffraction image. (b)–(e) Time-resolved diffraction images with listed times relative to impact time. The images show the temporal transition from cd phase Si to sh phase Si as the shock wave travels through the material. (f) Measured and simulated (solid line) sh diffraction peaks 406 ns after impact. The broad inner ring labeled PC is from the polycarbonate window and projectile.

measured diffraction peaks; the measured and simulated diffraction peaks are shown in Fig. 2(f) and agree very well both in peak position or shape and relative peak intensities. The lattice parameters used in the simulation are in good agreement with simple hexagonal lattice parameters determined for static compression of Si to a similar pressure [18]. Thus, we conclude that shocked Si (26 GPa impact stress followed by partial stress release to 19 GPa) remains crystalline rather than amorphous (as recently suggested in Ref. [23]) and transforms to a randomly oriented polycrystalline simple hexagonal structure.

The XRD results for shocked single-crystal Si in the constant 19 GPa state are shown in Fig. 3. The integrated diffracted intensities vs 2θ are shown in Figs. 3(a) and 3(d) for Si(100) and Si(111), respectively. The measured diffraction peak locations match simulations (solid lines) assuming a simple hexagonal structure with the same lattice parameters used for the simulation of the polycrystalline Si [Fig. 2(f)] indicating that the shocked single-crystal Si is also simple hexagonal with the same lattice parameters. However, the measured relative peak intensities do not match the simulation assuming randomly oriented grains, because the diffraction rings are highly localized, indicating that the high-pressure sh structure has significant preferred crystallographic orientation in the shocked state. These preferred orientation observations were used to relate the lattice orientations between the cd silicon and the high-pressure sh silicon structures, as discussed below.

The locations of the sh structure diffraction spots on the detector for the shocked single-crystal silicon provide important information regarding the orientation relations between the cd and sh structures. From each localized diffraction spot, a direction normal to the corresponding lattice plane of the sh structure can be calculated. However, this information is insufficient to fully specify the orientation relation between the cd and sh structures, because the sh lattice may be arbitrarily rotated around the normal direction while still producing the observed diffraction spot. For a single crystal, the observation of a diffraction spot from a different lattice plane would uniquely specify the orientation relation. For shocked single-crystal silicon, the orientation of the sh structure is degenerate with a number of different orientations of the sh phase depending on the transformation mechanism. Thus, we cannot be certain that two observed diffraction spots from different lattice planes correspond to a single sh orientation.

Because of the difficulties in directly extracting the orientation relations between the cd and sh structures from the measurements, a forward calculation was used to determine whether the data are consistent with a given trial orientation relation between the cd and sh structures. XRD simulations of the sh phase were performed assuming an orientation relation between the cd structure and the sh structure [26]. If the orientation relation assumed between the cd and sh structures in the simulation occurs in the shock experiments, the simulation should reproduce the measured diffraction spots; if multiple orientation relations occur, not all measured spots will be reproduced by the simulation. Furthermore, if the assumed orientation relations occur in the shock experiments, the simulation should not predict any additional diffraction spots that are not present in the measurements.

Simulations were performed for diffraction from the sh structure for both single-crystal experiments assuming 12 types of orientation relations linking high-symmetry directions between the cd and sh structures [26]. Only one set of orientation relations defined by $\langle 111\rangle_{cd} \| \langle 0001\rangle_{sh}$ and $\langle 10\bar{1}\rangle_{cd} \| \langle 10\bar{1}0\rangle_{sh}$ resulted in all simulated diffraction spots matching diffraction spots observed in both single-crystal experiments. The diffraction simulations with these orientation relations are shown in Figs. 3(c) and 3(f). For shock compression along $[100]_{cd}$, the six diffraction spots obtained from simulations were all present in the experiment. For shock compression along $[111]_{cd}$, all three

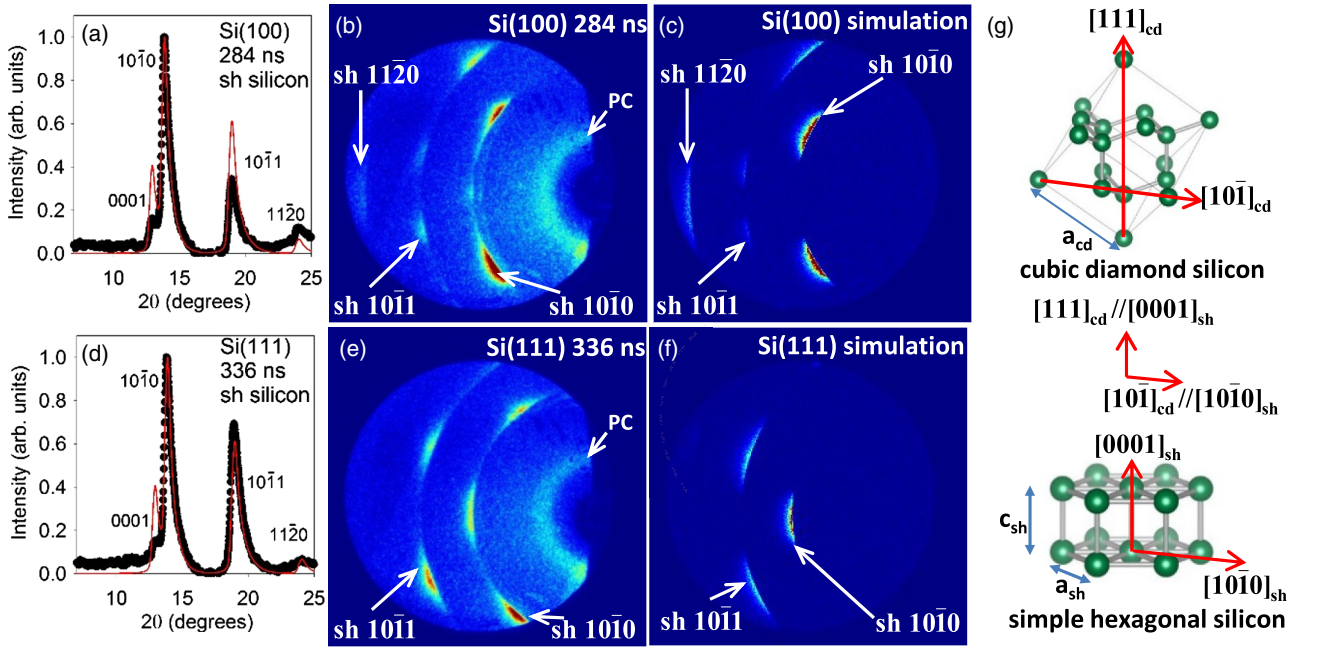

FIG. 3. X-ray diffraction results for shocked single-crystal silicon. (a)–(c) Results and simulations for Si(100) shocked to 19 GPa. (d)–(f) Results and simulations for Si(111) shocked to 19 GPa. One-dimensional integrated diffraction peaks in (a) and (d) match the peak locations for a simple hexagonal structure. The discrete nature of the measured diffraction rings in (b) and (e) indicate a significant preferred orientation for the high-pressure simple hexagonal structure. Simulations of the highly oriented simple hexagonal structure in (c) and (f) used the orientation relations between the ambient cubic diamond structure and the high-pressure simple hexagonal structure shown in (g).

diffraction spots (one $10\bar{1}0$ spot and two $10\bar{1}1$ spots) appearing in the simulation matched the measured diffraction spots. However, two additional bright $10\bar{1}0$ diffraction spots observed in the experiment on Si(111) and some additional weak diffraction spots observed in the experiment on Si(100) were not reproduced by the simulations, indicating that additional sh orientations are likely present. The relations for these additional orientations were not identified. However, other trial orientation relations were ruled out, because the predicted bright diffraction spots were not observed in the single-crystal experiments [26].

Our XRD measurements on shocked silicon single crystals and associated XRD simulation results suggest that the primary orientation relations between the cubic diamond and simple hexagonal structures are $\langle 111\rangle_{cd} \| \langle 0001\rangle_{sh}$ and $\langle 10\bar{1}\rangle_{cd} \| \langle 10\bar{1}0\rangle_{sh}$. To our knowledge, the atomic transformation mechanism and orientation relations between different polymorphs of silicon have neither been predicted directly by theory nor have they been determined previously from experiments. Instead, transformation mechanisms or orientation relations for structural changes in silicon have often been implicitly assumed [12,14,15,18,30–35]. For example, it has been suggested that the β-Sn structure can be obtained through continuous deformation with a large compression along a $\langle 100\rangle_{cd}$ direction and with isotropic expansion in the orthogonal plane [31–34]. Assuming this transformation pathway from the cd to β-Sn structure along with the commonly accepted transformation pathway from the β-Sn to sh structure [12,14,15,18,30,33] results in orientation relations between the cd and sh phases that are not compatible with our experimental findings. Because of the new results, past assumptions regarding atomic transformation pathways and orientation relations for structural changes in silicon need to be reexamined.

Recent MD simulations for germanium [36] and silicon [2,23,37] shocked along $[100]_{cd}$ have suggested that the transformation mechanisms for structural changes between the cd silicon and the β-Sn, *Imma*, and sh structures are more complex than commonly assumed [12,14,15,18,30–35]. An interesting finding of the MD simulations was that the transformations occurred along shear bands [2,36,37] which were attributed to planar stacking faults [36,37]. However, the MD simulations [2,36,37] predicted a peak state which was in a mixed phase rather than the completely transformed material. Additionally, the high-pressure structure determined from MD simulations for shocked Si(100) was identified as *Imma* [2] or amorphous [23]. These findings from the MD simulations are contradicted by our experimental results. Thus, the MD simulations need to be improved so that they can predict the structural transformation to the highly oriented sh phase observed in the experiments on shocked single-crystal silicon.

In summary, we have demonstrated that new experimental capabilities—now available at the DCS—can be used to examine the temporal evolution of structural changes in shock-compressed single-crystal and polycrystalline materials in real time. Analysis of the XRD results for shocked single-crystal silicon allowed us to make a good case for the primary orientation relations between the ambient cubic diamond silicon structure and the high-pressure simple hexagonal silicon structure. The ability to examine preferred orientations of high-pressure crystal structures in real time in shock-compression experiments can provide a wealth of new information regarding the atomistic transformation mechanisms occurring during stress-induced structural changes and also provides the data to assess the validity of MD simulations of compression-driven structural changes. Additionally, the ability to experimentally distinguish between amorphous and crystalline phases throughout the shock-compression and release process can address long-standing questions in planetary science: do geological materials such as quartz become amorphous during shock compression, or does amorphization occur upon stress release [38]?

Erik Zdanowicz helped design the target holder components and operated the two-stage gas gun during the experiments. Brendan Williams assisted with the target fabrication and the operation of the two-stage gas gun. Dan Paskvan assisted with data acquisition software. Tim Graber prepared the x-ray beam and measured the x-ray flux spectrum. This publication is based upon work performed at the Dynamic Compression Sector operated by Washington State University and supported by the Department of Energy (DOE), National Nuclear Security Administration (NNSA), under Award No. DE-NA0002442. This publication is also based upon work supported by the DOE NNSA under Award No. DE-NA0002007. This research used resources of the Advanced Photon Source, a U.S. Department of Energy (DOE) Office of Science User Facility operated for the DOE Office of Science by Argonne National Laboratory under Contract No. DE-AC02-06CH11357.

[1] Y. Shen, S. B. Jester, T. Qi, and E. J. Reed, Nat. Mater. **15**, 60 (2016).
[2] G. Mogni, A. Higginbotham, K. Gaal-Nagy, N. Park, and J. S. Wark, Phys. Rev. B **89**, 064104 (2014).
[3] D. Bancroft, E. L. Peterson, and S. Minshall, J. Appl. Phys. **27**, 291 (1956).
[4] G. E. Duvall and R. A. Graham, Rev. Mod. Phys. **49**, 523 (1977).
[5] T. d'Almeida and Y. M. Gupta, Phys. Rev. Lett. **85**, 330 (2000).
[6] S. J. Turneaure, Y. M. Gupta, and P. Rigg, J. Appl. Phys. **105**, 013544 (2009).
[7] D. H. Kalantar *et al.*, Phys. Rev. Lett. **95**, 075502 (2005).
[8] J. Hawreliak *et al.*, Phys. Rev. B **74**, 184107 (2006).
[9] http://www.dcs-aps.wsu.edu/.
[10] A. Mujica, A. Rubio, A. Munoz, and R. J. Needs, Rev. Mod. Phys. **75**, 863 (2003).
[11] J. C. Jamieson, Science **139**, 762 (1963).
[12] M. I. McMahon, R. J. Nelmes, N. G. Wright, and D. R. Allan, Phys. Rev. B **50**, 739 (1994).
[13] G. Shen, D. Ikuta, S. Sinogeikin, Q. Li, Y. Zhang, and C. Chen, Phys. Rev. Lett. **109**, 205503 (2012).
[14] R. J. Needs and R. M. Martin, Phys. Rev. B **30**, 5390 (1984).
[15] S. P. Lewis and M. L. Cohen, Phys. Rev. B **48**, 16144 (1993).
[16] J. Z. Hu and I. L. Spain, Solid State Commun. **51**, 263 (1984).
[17] H. Olijnyk, S. K. Sikka, and W. B. Holzapfel, Phys. Lett. A **103**, 137 (1984).
[18] J. Z. Hu, L. D. Merkle, C. S. Menoni, and I. L. Spain, Phys. Rev. B **34**, 4679 (1986).
[19] M. Hanfland, U. Schwarz, K. Syassen, and K. Takemura, Phys. Rev. Lett. **82**, 1197 (1999).
[20] W. H. Gust and E. B. Royce, J. Appl. Phys. **42**, 1897 (1971).
[21] T. Goto, T. Sato, and Y. Syono, Jpn. J. Appl. Phys. **21**, L369 (1982).
[22] S. J. Turneaure and Y. M. Gupta, Appl. Phys. Lett. **91**, 201913 (2007).
[23] S. Zhao *et al.*, Extreme Mechanics Lett. **5**, 74 (2015).
[24] D. H. Kalantar *et al.*, Rev. Sci. Instrum. **70**, 629 (1999).
[25] A. Loveridge-Smith *et al.*, Phys. Rev. Lett. **86**, 2349 (2001).
[26] See Supplemental Material at http://link.aps.org/supplemental/10.1103/PhysRevLett.117.045502, which includes Refs. [27–29], for additional experimental details and results, methods used to reduce two-dimensional x-ray diffraction images to one-dimensional diffraction peaks, methods used for powder diffraction simulations, and methods used for and results of diffraction simulations of textured simple hexagonal silicon with particular orientation relations relative to the cubic diamond structure.
[27] S. P. Marsh, *LASL Shock Hugoniot Data* (University of California, Berkeley, 1980).
[28] A. P. Hammersley, ESRF Internal Report No. ESRF97-HA02T, 1997.
[29] A. P. Hammersley, S. O. Svensson, M. Hanfland, A. N. Fitch, and D. Hausermann, High Press. Res. **14**, 235 (1996).
[30] S. M. Sharma and S. K. Sikka, J. Phys. Chem. Solids **46**, 477 (1985).
[31] K. Gaal-Nagy, A. Bauer, P. Pavone, and D. Strauch, Comput. Mater. Sci. **30**, 1 (2004).
[32] K. Gaal-Nagy and D. Strauch, Phys. Rev. B **73**, 134101 (2006).
[33] H. Katzke, U. Bismayer, and P. Toledano, Phys. Rev. B **73**, 134105 (2006).
[34] S. L. Qui and P. M. Marcus, J. Phys. Condens. Matter **24**, 225501 (2012).
[35] G. T. Hohensee, M. R. Fellinger, D. R. Trinkle, and D. G. Cahill, Phys. Rev. B **91**, 205104 (2015).
[36] J. M. D. Lane and A. P. Thompson, *AIP Conf. Proc.* 1195, 1157 (2009).
[37] J. M. D. Lane, A. P. Thompson, and T. J. Vogler, Phys. Rev. B **90**, 134311 (2014).
[38] S. N. Luo, T. J. Ahrens, and P. D. Asimow, J. Geophys. Res. **108**, 2421 (2003).